Dysonian Electron-Spin-Resonance Spectra of Local Magnetic Moments in Metals

David C. Johnston
Ames Laboratory and Department of Physics and Astronomy, Iowa State University, Ames, Iowa 50011, USA
(Dated: December 14, 2024)

The absorptive and dispersive components of the frequency-dependent magnetic susceptibility both contribute to the electron-spin resonance (ESR) radio-frequency (rf) power absorption of local magnetic moments in metals according to Dyson's theory. The magnetic-field prefactor present in the expression for this power absorption has been omitted in the past when fitting Dyson's lineshape to the observed field derivative of broad ESR rf power absorption spectra but is shown here to significantly influence such fits and therefore also the quantitative physical interpretations of the temperature-dependent fit parameters.

In both nuclear (NMR) [1, 2] and electron spin (ESR) [3–6] magnetic resonance and relaxation, the Bloch equations are often the starting point for analyzing experimental data. The Bloch equations give the Cartesian components of the magnetization $\mathbf{M}$ per unit volume, which is precessing around the magnetic field $\mathbf{H}$, as [7]

$$\frac{dM_x}{dt} = -\gamma(\mathbf{M}\times\mathbf{H})_x - M_x/T_2, \quad (1a)$$

$$\frac{dM_y}{dt} = -\gamma(\mathbf{M}\times\mathbf{H})_y - M_y/T_2, \quad (1b)$$

$$\frac{dM_z}{dt} = -\gamma(\mathbf{M}\times\mathbf{H})_z + (M_0 - M_z)/T_1, \quad (1c)$$

where t is the time, the negative sign prefactors arise from the negative charge on the electron appropriate for ESR, T_2 is the transverse spin-spin relaxation (decoherence) time, M_0 is the thermal-average magnetization (magnetic moment per unit volume) when the magnetization is aligned in the direction of the applied magnetic field

$$\mathbf{H} = H_0\hat{\mathbf{k}}, \quad (2)$$

T_1 is the longitudinal relaxation time associated with decay of the magnetic energy, and γ is the gyromagnetic ratio of the moment ($\gamma = g\mu_B/\hbar$ for Heisenberg spins, g is the spectroscopic splitting factor, μ_B is the Bohr magneton, and $\hbar$ is Planck's constant divided by 2π). The Gaussian cgs system of units is used in this paper, with the exception of the expression for the skin depth δ which is expressed later in SI units. The damping terms on the far right sides of Eqs. (1) are phenomenologically introduced so that the relaxation of each of the Cartesian components of $\mathbf{M}$ in a free-induction decay experiment is exponential, as predicted by quantum statistics and often observed experimentally.

In the absence of damping ($T_1,\ T_2 \to \infty$) and additional magnetic fields, the Bloch equations yield a magnetization that precesses around $\mathbf{H}$ at angular frequency $\omega_0 = \gamma H_0$ according to

$$M_x = M_0 \sin\theta\cos(\omega_0 t), \quad (3a)$$

$$M_y = M_0 \sin\theta\sin(\omega_0 t), \quad (3b)$$

$$M_z = M_0\cos\theta, \quad (3c)$$

where θ is the constant angle that $\mathbf{M}$ makes with the z axis.

For magnetic resonance experiments, an additional radio-frequency (rf) magnetic field $\mathbf{H}_1$ with angular frequency ω is present that is usually taken to be linearly polarized along the x axis, which can be considered to be a superposition of a circularly-polarized magnetic field that has a precession angular velocity parallel to the z axis as does $\mathbf{M}$ and a counter-rotating field that has a precession angular velocity antiparallel to the z axis, i.e.,

$$\mathbf{H}_1 = -2H_1\cos(\omega t)\hat{\mathbf{i}} \quad (4a)$$

$$= -H_1[\cos(\omega t)\hat{\mathbf{i}} + \sin(\omega t)\hat{\mathbf{j}}] \quad (4b)$$

$$- H_1[\cos(\omega t)\hat{\mathbf{i}} - \sin(\omega t)\hat{\mathbf{j}}], \quad (4c)$$

where the negative sign prefactors are due to the negative charge on the electron that apply to ESR as in Eqs. (1). For narrow absorption lines, the counter-rotating component of $\mathbf{H}_1$ makes no significant contribution to the observed rf power absorption and is therefore usually ignored. However, for wide ESR spectra with widths of the order of H_0, the influence of the counter-rotating component (4c) of $\mathbf{H}_1$ must also be taken into account.

In a primed reference frame where the $x'y'$ plane is rotating in the same direction as $\mathbf{M}$ according to Eq. (4b), but with the angular speed ω instead of ω_0, the steady-state solutions of the Bloch equations (1) to first order in H_1 (nonsaturating condition) are [3]

$$M_{x'} = \frac{\gamma H_1(\omega_0-\omega)T_2^2}{1+(\omega_0-\omega)^2T_2^2}M_0, \quad (5a)$$

$$M_{y'} = \frac{-\gamma H_1 T_2}{1+(\omega_0-\omega)^2T_2^2}M_0, \quad (5b)$$

$$M_{z'} = M_0. \quad (5c)$$

These expressions give the magnitude $M = M_0$ to first order in H_1, as expected. However, to second order in H_1 one obtains the unphysical result $M > M_0$, which illustrates a limitation of the Bloch equations. The equality $M = M_0$ is predicted by the Bloch equations for free-induction decay experiments at times $t = 0$ and $t \to \infty$, but at intermediate times one obtains $M = M_0\sqrt{e^{-2t/T_2} + (1-e^{-t/T_1})^2} < M_0$ for $T_2/T_1 \lesssim 2$ due to the transverse decoherence of the precessing magnetic moments associated with T_2 [8]. This reduction is especially pronounced for $T_2/T_1 \ll 1$. One has the phys-

ical limit $T_2/T_1 \lesssim 2$ in order that $M \leq M_0$ for all times during free-induction decay [8].

The dispersive $[\chi'(\omega)]$ and absorptive $[\chi''(\omega)]$ components of the steady-state magnetic susceptibility to first order in H_1 are obtained from Eqs. (5a) and (5b) as [3]

$$\chi'(\omega) \equiv \frac{M_{x'}}{H_1} = \frac{(\omega_0-\omega)T_2^2}{1+(\omega_0-\omega)^2T_2^2}\gamma M_0, \quad (6a)$$

$$\chi''(\omega) \equiv -\frac{M_{y'}}{H_1} = \frac{T_2}{1+(\omega_0-\omega)^2T_2^2}\gamma M_0. \quad (6b)$$

$\chi''(\omega)$ is a Lorentzian function, for which the half width at half maximum peak intensity (HWHM) is $1/T_2 \equiv \Delta\omega$. With this assignment, Eqs. (6) become

$$\chi'(\omega) = \frac{\omega_0-\omega}{\Delta\omega^2+(\omega_0-\omega)^2}\gamma M_0, \quad (7a)$$

$$\chi''(\omega) = \frac{\Delta\omega}{\Delta\omega^2+(\omega_0-\omega)^2}\gamma M_0. \quad (7b)$$

Broadening of the ESR spectrum occurs due to the magnetic dipole interaction between spins in systems with high concentrations of local moments, resulting in a non-Lorentzian lineshape. However, the exchange interaction between the spins gives rise to narrowing of the resonance, leading again to a Lorentzian lineshape [3].

In order to take into account the influence of the counter-rotating component of $\mathbf{H}_1$ in Eq. (4c) that is necessary to fit broad absorption spectra, one adds an additional term to each of Eqs. (7) where $-\omega$ is substituted for ω, yielding

$$\chi'(\omega) = \gamma M_0\left[\frac{\omega_0-\omega}{\Delta\omega^2+(\omega_0-\omega)^2}+\frac{\omega_0+\omega}{\Delta\omega^2+(\omega_0+\omega)^2}\right], \quad (8a)$$

$$\chi''(\omega) = \gamma M_0\left[\frac{\Delta\omega}{\Delta\omega^2+(\omega_0-\omega)^2}+\frac{\Delta\omega}{\Delta\omega^2+(\omega_0+\omega)^2}\right]. \quad (8b)$$

ESR in metals was studied theoretically by Dyson in 1955 [9] and his predictions were first utilized to interpret experimental conduction-electron spin-resonance data by Feher and Kip [10]. Another case of Dyson's theory describes ESR of well-defined local magnetic moments in metals, where the Dysonian absorption susceptibility $\chi''_{\rm D}(\omega)$ contains a contribution from $\chi'(\omega)$ given by [9]

$$\chi''_{\rm D}(\omega) = \chi''(\omega) - \alpha\chi'(\omega), \quad (9)$$

where $0 \leq \alpha \leq 1$ with $\alpha = 0$ or 1 if the rf skin depth δ is much larger or much smaller than the sample dimension that is perpendicular to the linearly polarized $\mathbf{H}_1$ in Eq. (4a), respectively. The expression for δ is

$$\delta({\rm m}) = \sqrt{\frac{\rho(\Omega\ {\rm m})}{\pi f({\rm Hz})\mu({\rm H/m})}} \qquad ({\rm SI\ units}), \quad (10)$$

where ρ is the electrical resisitivity, f is the rf frequency, and μ is the magnetic permeability of the sample [11]. Substituting Eqs. (8) into (9) gives

$$\chi''_{\rm D}(\omega) = \gamma M_0\left[\frac{\Delta\omega-\alpha(\omega_0-\omega)}{\Delta\omega^2+(\omega_0-\omega)^2}+\frac{\Delta\omega-\alpha(\omega_0+\omega)}{\Delta\omega^2+(\omega_0+\omega)^2}\right]. \quad (11)$$

ESR of local magnetic moments in metals can only be observed for a limited range of local moments [4], such as for the S-state ions Gd^{+3} and Eu^{+2} with electron configurations $4f^7$ and spin $S = 7/2$ and orbital angular momentum $L = 0$, where the resonance is observed even in concentrated alloys and compounds. ESR of the Kramers ions Dy^{+3}, Er^{+3}, and Yb^{+3} in alloys and compounds have also been observed. Among the $3d$ transition elements, ESR spectra of Mn^{+2} with electron configuration $3d^5$ with $S = 5/2$ have also been obtained. Generally fine and hyperfine structures are not resolved in the ESR spectra for high concentrations of these ions in metallic alloys and compounds, where broad featureless Lorentzian-like resonances are observed instead.

ESR slow-passage experiments involve keeping ω fixed and slowly varying the applied static field H_0. Here, $\omega = \gamma H$, $\omega_{\rm res} = \gamma H_{\rm res}$, and $H_{\rm res}$ is the resonant field that can be different from H_0 due to the presence of internal and demagnetizing fields discussed in Ref. [12]. Using these conversions Eq. (11) becomes [13, 14]

$$\chi''_{\rm D}(H) = \chi_0|H|\left[\frac{\Delta H-\alpha(H_{\rm res}-H)}{\Delta H^2+(H_{\rm res}-H)^2}+\frac{\Delta H-\alpha(H_{\rm res}+H)}{\Delta H^2+(H_{\rm res}+H)^2}\right], \quad (12)$$

where $\chi_0 \equiv M(H)/H$ is the dimensionless volume susceptibility. Here, ΔH is the half width in field at half-maximum Lorentzian peak height. The value of $\chi''_{\rm D}(H = 0)$ in the paramagnetic state obtained from Eq. (12) is zero. The H prefactor is analogous to the ω prefactor in the expression for the time-averaged power absorbed by a driven, damped, simple-harmonic oscillator.

The time-average power $P(H,T)$ absorbed in steady state by a metallic sample containing local magnetic moments from the ESR rf magnetic field is [1–3, 6, 10]

$$P(H,T) = F(H,T)\chi''_{\rm D}(H), \quad (13a)$$

where

$$F(H,T) = \frac{\gamma H_1^2 H_{\rm res}}{8}[A\delta(H,T)] \quad (13b)$$

and A is the area of a surface of the sample parallel to the linearly-polarized applied rf field $\mathbf{H}_1$. The integral $\int_0^\infty e^{-x/\delta}dx = \delta$, so the factor $A\delta(H,T)$ in Eq. (13b) is the volume of the sample beneath the area A that is exposed to the rf field $\mathbf{H}_1$. Due to the $|H|$ prefactor in $P(H,T)$, the integral $\int_0^H P(H',T)dH'$ diverges logarithmically with increasing H for $H \gg H_{\rm res}$. However, experimental spectra are usually limited to $H \lesssim 2H_{\rm res}$.

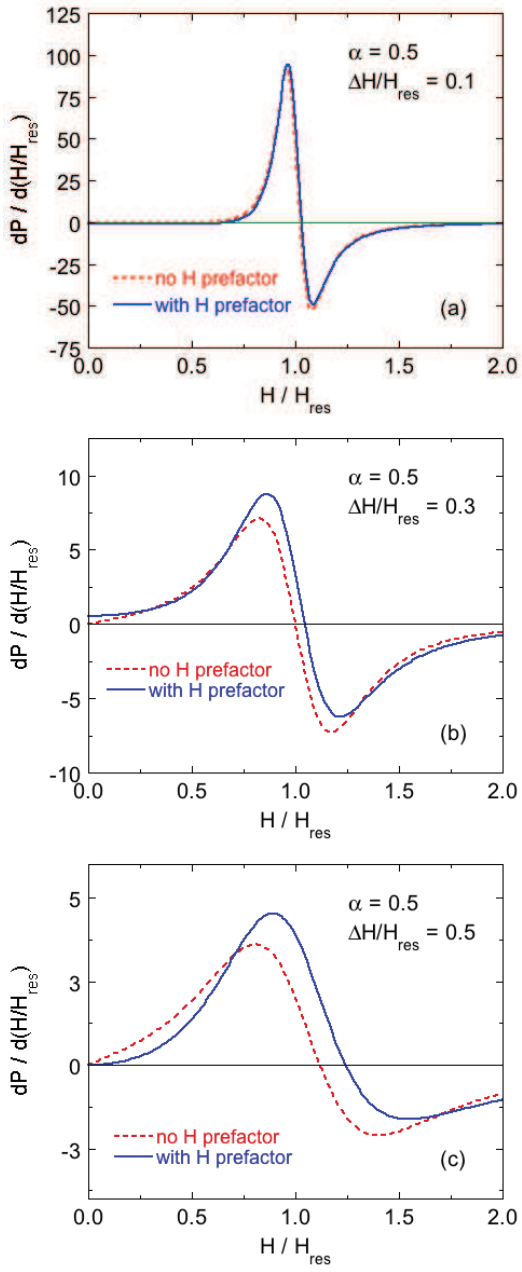

FIG. 1: Derivative of the absorbed rf power P with respect to $\tilde{H} = H/H_{\rm res}$ in arbitrary units for the ratio $\alpha = 0.5$ of the dispersive to the absorptive components of the Dysonian absorptive susceptibility with (a) $\Delta H/H_{\rm res} = 0.1$, (b) 0.3, and (c) 0.5, each both with and without the $\tilde{H}$ prefactor in Eq. (16), where ΔH is the half width at half height of the Lorentzian functions in Eq. (12) and $H_{\rm res}$ is the resonant field.

In this paper, the prefactor H in Eq. (12) is demonstrated to be important to fits of broad ESR absorption spectra of local moments in metals. To facilitate plotting the calculated ESR spectra, $H_{\rm res}$, H and ΔH are normalized by $H_{\rm res}$ thus yielding the dimensionless parameters

$$\tilde{H}_{\rm res} = 1, \qquad \tilde{H} = \frac{H}{H_{\rm res}}, \qquad \Delta\tilde{H} = \frac{\Delta H}{H_{\rm res}}. \tag{14}$$

Then Eq. (12) becomes

$$\chi''_{\rm D}(\tilde{H}) \;=\; \chi_0|\tilde{H}|\left[\frac{\Delta\tilde{H}-\alpha(1-\tilde{H})}{\Delta\tilde{H}^2+(1-\tilde{H})^2} + \frac{\Delta\tilde{H}-\alpha(1+\tilde{H})}{\Delta\tilde{H}^2+(1+\tilde{H})^2}\right]. \tag{15}$$

Experimentally, to improve the signal to noise ratio an ac modulation of $\mathbf{H}$ is used so the observed derivative absorption spectrum is obtained from Eqs. (13) and (15) as

$$\frac{dP(\tilde{H})}{d\tilde{H}} \propto \frac{d\chi''_{\rm D}(\tilde{H})}{d\tilde{H}}. \tag{16}$$

$P(\tilde{H})$ is even in $\tilde{H}$ as required physically, and $dP(\tilde{H})/d\tilde{H}$ is odd in $\tilde{H}$.

Shown in Fig. 1 are plots of $dP(\tilde{H})/d\tilde{H}$ versus $\tilde{H}$ according to Eqs. (15) and (16) for a typical $\alpha = 0.5$ and reduced Lorentzian half widths $\Delta\tilde{H}$ of 0.1, 0.3 and 0.5, where each panel shows the results both with and without the $\tilde{H}$ prefactor on the right side of Eq. (15). The $\tilde{H}$ prefactor is seen to have a significant influence on both the shape and amplitude of the derivative curves.

The so-called A/B ratio (the height of the first peak divided by that of the second peak in derivative spectra such as shown in Fig. 1) is also affected by the presence of the $\tilde{H}$ prefactor on the right side of Eq. (15) as shown by plots of A/B versus α in Fig. 2 for $\Delta\tilde{H}$ values from 0.02 to 0.5. One sees from Fig. 2(b) that the α dependence of A/B depends rather strongly on $\Delta\tilde{H}$ when the $\tilde{H}$ prefactor in Eq. (15) is included. On the other hand, if the prefactor is not included, the A/B ratio is not very sensitive to $\Delta\tilde{H}$ as shown in Fig. 2(a) and for $\Delta\tilde{H} \ll 1$ has a value of 1 for $\alpha = 0$ and ≈ 2.55 for $\alpha = 1$ [5].

The ratio of the peak-to-peak linewidth $H_{\rm pp}$ in the field-derivative spectra to the Lorentzian half width ΔH in Eq. (12) is plotted versus α in Fig. 3 without [Fig. 3(a)] and with [Fig. 3(b)] the $\tilde{H}$ prefactor in Eq. (15) for $\Delta\tilde{H}$ values from 0.02 to 0.5. Here the influence of $\Delta\tilde{H}$ is seen to be minimal in the absence of the $\tilde{H}$ prefactor, whereas when the prefactor is included, strong influences are seen in the $\Delta\tilde{H}$ dependence of $\Delta H_{\rm pp}/\Delta H$ on α.

The above results are relevant to many recently published X-band (~ 9.5 GHz) ESR field-derivative power-absorption spectra with broad featureless lineshapes for local moments in metallic compounds that were fitted by Dysonian-type lineshapes. For example, Mn ESR data on $LaMnO_3$ were fitted by $\alpha \approx 0$ and $\Delta H/H_{\rm res} \sim 0.7$ [13]. An ESR study of the Eu^{+2} resonance in $EuFe_2As_2$ yielded $\Delta H/H_{\rm res} = 0.57$ at $T = 300$ K [15]. Similar results were obtained at $T = 300$ K for Co-substituted $EuFe_{2-x}Co_xAs_2$ [16], for Eu^{+2}-doped $Ba_{1-x}Eu_xFe_2As_2$ with $x = 0.20$, 0.55 and 0.95 [17], and for Ru-substituted $EuFe_{2-x}Ru_xAs_2$ [18]. Linewidths of $\sim 0.3H_{\rm res}$ were observed from ~ 100 to 300 K for Eu^{+2} in an EuB_6 crystal [19]. ESR spectra of Gd^{+3} in Gd_2PdSi_3 gave $\Delta H/H_{\rm res} \gtrsim$

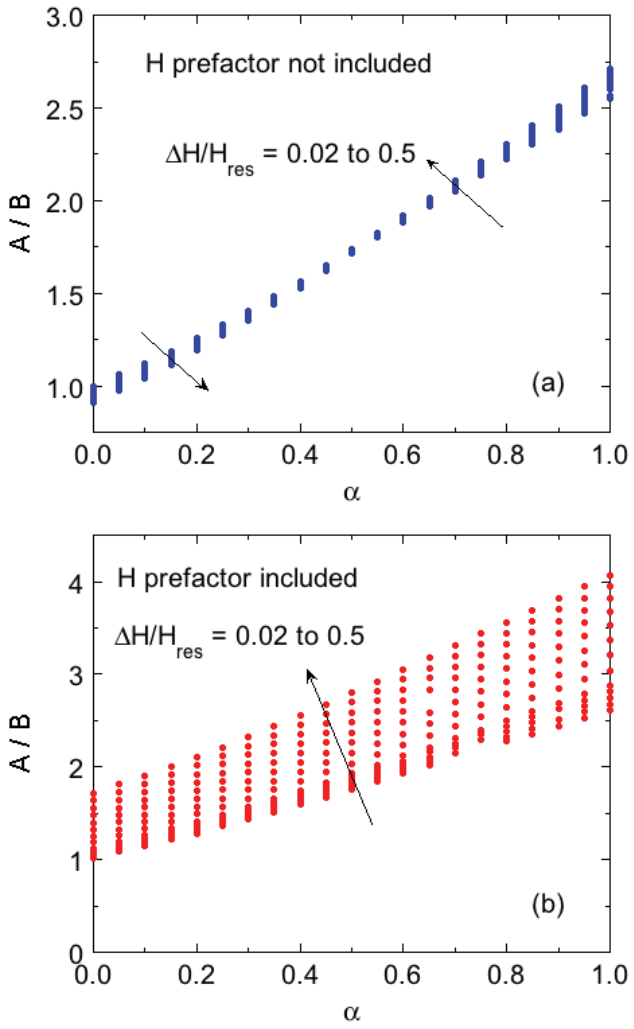

FIG. 2: A/B ratio of the field derivative of the rf power-absorption spectrum versus α for $\Delta\tilde{H} \equiv \Delta H/H_{\rm res} = 0.02$, 0.04, ..., 0.10, 0.15, ..., 0.5 (a) without the $\tilde{H}$ prefactor in Eq. (16) present and (b) with the $\tilde{H}$ prefactor included. Whereas the dependence of A/B versus α on $\Delta H/H_{\rm res}$ is rather weak if the $\tilde{H}$ prefactor is not included, the dependence is quite strong when the prefactor is included. Note the different ordinate scales in (a) and (b).

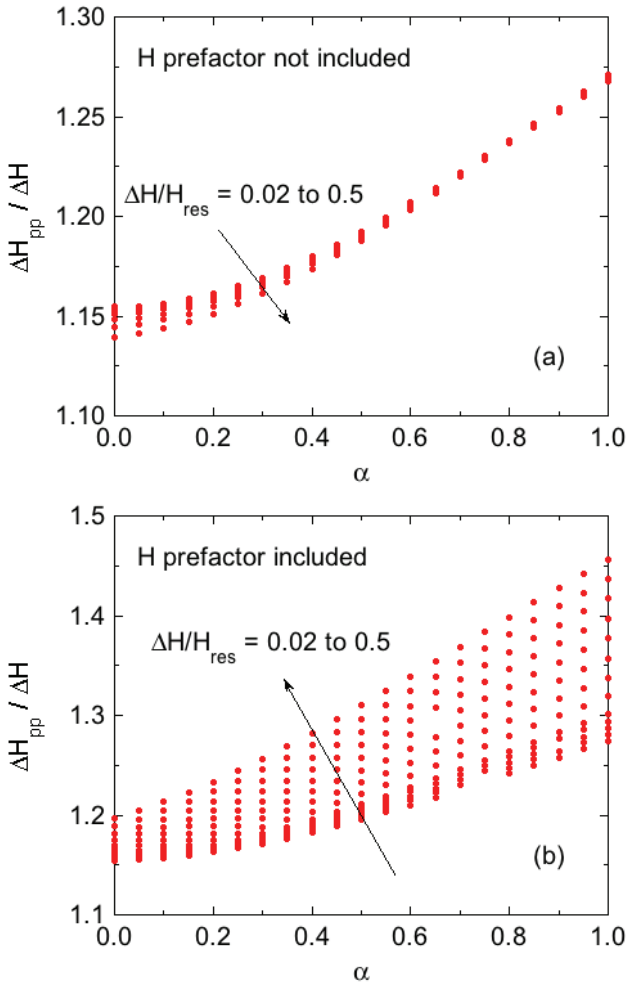

FIG. 3: Ratio $\Delta H_{\rm pp}/\Delta H$ of the peak-to-peak linewidth of the field-derivative of the rf power-absorption spectrum divided by the Lorentzian half width at half peak intensity versus α for $\Delta\tilde{H} \equiv \Delta H/H_{\rm res} = 0.02$, 0.04, ..., 0.10, 0.15, ..., 0.5 (a) without the $\tilde{H}$ prefactor in Eq. (16) and (b) with the prefactor present. As in Fig. 2, including the $\tilde{H}$ prefactor is seen to have a strong influence on the results. Note the different ordinate scales in (a) and (b).

0.3 [20]. The Gd^{+3} ESR spectra at $T = 4.2$ K for 2% Gd-doped $Ce(Cu_{0.5}Ni_{0.5})_2Ge_2$ yielded $\Delta H/H_{\rm res} \sim 1$ [21] and for 2% Gd-doped YNi_2B_2C at $T = 16$–55 K gave $\Delta H/H_{\rm res} \sim 0.3$ [22].

In summary, it was shown that including the multiplicative H prefactor in Eq. (12) in the field derivative of the Dysonian rf power absorption spectrum of local magnetic moments in metals has a substantial influence on the lineshape and amplitude of the observed field derivative of broad ESR spectra. This prefactor has long been known to be present [1–3, 6, 10] but has not been included in the past to our knowledge when fitting such experimental ESR spectra. For example, a comparison of the ESR fitting parameters α, ΔH and $H_{\rm res}$ determined with and without the H prefactor in Eq. (12) was recently carried out of the T-dependent broad X-band field-derivative ESR spectra [23] for the metallic compound $EuCo_{2-y}As_2$ [24]. The parameters ΔH and $H_{\rm res}$ were found to differ by only few percent between the two fits, whereas without the H prefactor α was found to be a factor of 2–3 too large with some unphysical values $\alpha > 1$. In addition, as pointed out below Eq. (13), the field-integrated power absorption diverges for $H \to \infty$ when the theoretically-required H prefactor is present but attains an incorrect value of $\pi\chi_0$ in this limit when the prefactor is omitted.

Acknowledgments

The author is grateful to Q.-P. Ding, Y. Furukawa, and N. S. Sangeetha for helpful discussions. This research was supported by the U. S. Department of Energy, Office of Basic Energy Sciences, Division of Materials Sciences and Engineering. Ames Laboratory is operated for the U. S. Department of Energy by Iowa State University under Contract No. DE-AC02-07CH11358.

[1] A. Abragam, *Principles of Nuclear Magnetism* (Clarendon, Oxford, 1961).
[2] C. P. Slichter, *Principles of Magnetic Resonance* (Harper & Row, New York, 1963).
[3] G. E. Pake and T. L. Estle, *The Physical Principles of Electron Paramagnetic Resonance*, 2nd edition (Benjamin, Reading, MA, 1973).
[4] R. H. Taylor, Electron spin resonance of magnetic ions in metals—An experimental review, Adv. Phys. **24**, 681 (1975).
[5] S. E. Barnes, Theory of electron spin resonance of magnetic ions in metals, Adv. Phys. **30**, 801 (1981).
[6] C. P. Poole, Jr., *Elecron Spin Resonance*, 2nd edition (Wiley, New York, 1983).
[7] F. Bloch, Nuclear Induction, Phys. Rev. **70**, 460 (1946).
[8] Q.-P. Ding, private communication.
[9] F. J. Dyson, Electron Spin Resonance Absorption in Metals. II. Theory of Electron Diffusion and the Skin Effect, Phys. Rev. **98**, 349 (1955).
[10] G. Feher and A. F. Kip, Electron Spin Resonance Absorption in Metals. I. Experimental, Phys. Rev. **98**, 337 (1955).
[11] The magnetic permeability in SI units is given by $\mu = \mu_0[1 + (M/H)]$, where μ_0 is the magnetic permeability of free space. M is the magnetization of the sample per unit volume and the dimensionless ratio $M(T, H)/H$ can be dependent on the temperature T and the magnitude and direction of the applied field **H**. The required SI value of M/H is obtained from M/H in dimensionless cgs units of G/Oe via M/H (SI) $= (4\pi)^{-1}(M/H)$ (cgs).
[12] D. C. Johnston, Magnetic dipole interactions in crystals, Phys. Rev. B **93**, 014421 (2016).
[13] V. A. Ivanshin, J. Deisenhofer, H.-A. Krug von Nidda, A. Loidl, A. A. Mukhin, A. M. Balbashov, and M. V. Eremin, ESR study in lightly doped $La_{1-x}Sr_xMnO_3$, Phys. Rev. B **61**, 6213 (2000).
[14] J. P. Joshi and S. V. Bhat, On the analysis of broad Dysonian electron paramagnetic resonance spectra, J. Magn. Res. **168**, 284 (2004). In this paper, ΔH is the full width at half maximum Lorentzian peak height instead of the half width at half maximum used in the present paper and in Ref. [13].
[15] E. Dengler, J. Deisenhofer, H.-A. Krug von Nidda, S. Khim, J. S. Kim, K. H. Kim, F. Casper, C. Felser, and A. Loidl, Strong reduction of the Korringa relaxation in the spin-density wave regime of $EuFe_2As_2$ observed by electron spin resonance, Phys. Rev. B **81**, 024406 (2010).
[16] H.-A. Krug von Nidda, S. Kraus, S. Schaile, E. Dengler, N. Pascher, M. Hemmida, M. J. Eom, J. S. Kim, H. S. Jeevan, P. Gegenwart, J. Deisenhofer, and A. Loidl, Electron spin resonance in Eu-based iron pnictides, Phys. Rev. B **86**, 094411 (2012).
[17] P. F. S. Rosa, C. Adriano, W. Iwamoto, T. M. Garitezi, T. Grant, Z. Fisk, and P. G. Pagliuso, Evolution of Eu^{2+} spin dynamics in $Ba_{1-x}Eu_xFe_2As_2$, Phys. Rev. B **86**, 165131 (2012).
[18] M. Hemmida, H.-A. Krug von Nidda, A. Günther, A. Loidl, A. Leithe-Jasper, W. Schnelle, H. Rosner, and J. Sichelschmidt, Probing the density of states in $EuFe_{2-x}Ru_xAs_2$, Phys. Rev. B **90**, 205105 (2014).
[19] R. R. Urbano, P. G. Pagliuso, C. Rettori, S. B. Oseroff, J. L. Sarrao, P. Schlottmann, and Z. Fisk, Magnetic polaron and Fermi surface effects in the spin-flip scattering of EuB_6, Phys. Rev. B **70**, 140401(R) (2004).
[20] J. Deisenhofer, H.-A. Krug von Nidda, A. Loidl, and E. V. Sampathkumaran, ESR investigation of the spin dynamics in $(Gd_{1-x}Y_x)_2PdSi_3$, Solid State Commun. **125**, 327 (2003).
[21] H. A. Krug von Nidda, A. Schütz, M. Heil, B. Elschner, and A. Loidl, Electron-spin-resonance investigation of the heavy-fermion compound $Ce(Cu_{1-x}Ni_x)_2Ge_2$, Phys. Rev. B **57**, 14 344 (1998).
[22] P. G. Pagliuso, C. Rettori, S. B. Oseroff, P. C. Canfield, E. M. Baggio-Saitovich, and D. Sanchez, Electron spin resonance of Gd^{3+} in the normal state of RNi_2B_2C (R = Y, Lu), Phys. Rev. B **57**, 3668 (1998).
[23] N. S. Sangeetha, V. K. Anand, E. Cuervo-Reyes, V. Smetana, A.-V. Mudring, and D. C. Johnston, Enhanced moments of Eu in single crystals of the metallic helical antiferromagnet $EuCo_{2y}As_2$, Phys. Rev. B **97**, 144403 (2018).
[24] N. S. Sangeetha, S. D. Cady, and D. C. Johnston, Electron-spin resonance of Eu^{+2} spins in metallic $EuCo_{2-y}As_2$ single crystals, (unpublished).